5607

Broad Acting Glutamine Antagonism Remodels the Tumor Microenvironment; Induces Distinctive Immune Modulation; and, Synergizes with Immune Checkpoint Blockade

Yumi Yokoyama, Ph.D. and Robert Wild, Ph.D.
Dracen Pharmaceuticals Inc., 780 Third Ave, 45th Floor, New York, NY 10017

Summary

DRP-104, a novel broad acting glutamine antagonist, has significant therapeutic potential in cancer via directly targeting tumor metabolism and inducing a potent antitumor immune response. Here we sought to elucidate the immunomodulatory effect of DRP-104 on tumor growth inhibition as a single agent and in combination with PD-1/PD-L1 checkpoint inhibitors in syngeneic models. We utilized multiple technologies to assess mechanistic effects on immune cells *in vivo* including flowcytometry, multiplex immunoassay, gene expression profiling and GeoMx™ digital spatial profiling.

DRP-104 mediated tumor growth inhibition was associated with increased tumor-infiltrating leukocytes (TIL) including T, NKT, and NK cells, M1-polarized tumor associated macrophages, and decreased immune-suppressive cells such as MDSCs. Nanostring® IO360 analysis revealed broad immunological modulation such as increase in cytotoxicity/antigen presentation score; increase in tumor metabolic stress/apoptotic score; and decrease in cell proliferation score. GeoMx® profiling also demonstrated increased tumoral T cells and granzyme B expression. DRP-104 showed significant tumor growth inhibition and regressions as a single agent in mouse syngeneic tumor models, including those resistant to immune checkpoint inhibitors. Lastly, combination of DRP-104 with anti-PD-1 Ab or anti-PD-L1 Ab further improved survival effect with long-term durable cures.

In summary, DRP-104 treatment resulted in broad remodeling of the tumor microenvironment including increased infiltration and function of multiple immune cells distinct from activities obtained by a checkpoint inhibitor treatment. Combination therapy of DRP-104 with anti-PD-1/PD-L1 achieved significantly increased anti-tumor efficacy including long-term durable cures even in checkpoint inhibitor resistant models. This unique and non-overlapping mechanism of action supports clinical development of DRP-104 alone and in combination with PD-1/PD-L-1 checkpoint inhibitors.

Background

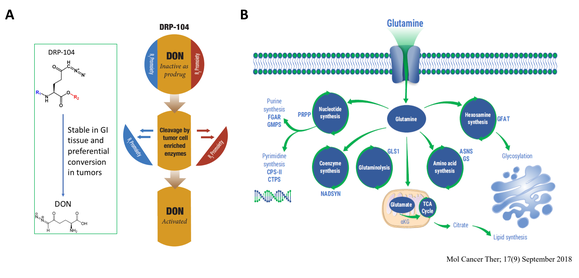

Figure 1. A. DRP-104 is a prodrug of the broad acting glutamine antagonist DON (6-Diazo-5-oxo-L-norleucine). DRP-104 is inactive in its prodrug form with high plasma and GI tissue stability. DRP-104 is preferentially distributed in tumors where it is bio-transformed and activated to the active moiety DON. **B.** Multiple glutamine dependent pathways are inhibited by DON.

DRP-104 Achieves 66x Tumor/Plasma Exposure Ratios for DON in CES-1 KO Mice Providing PoC for Prodrug Tumor Targeting *In Vivo*

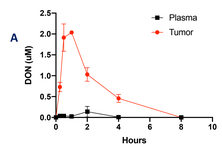

B

	Tumor	Plasma	Tumor/Plasma
C_{max} (µmol/L)	2.037	0.039	52.5
$AUC_{0-\infty}$ (µmol/L*h)	4.428	0.067	65.6

Figure 2. CES-1 ko mice (C57BL/6 CES1-/-) bearing MC38 tumors in the flank were dosed *s.c.* in the opposite flank with DRP-104 (2.6 mg/kg). Tumor and plasma were harvested 0.25-8 hr after the administration to calculate $AUC_{0-\infty}$. $AUC_{0-\infty}$ (µmol.h/ml) was calculated by the macro PK Functions for Microsoft Excel. **A.** DON concentration in tumor and plasma. **B.** DON $AUC_{0-\infty}$ and C_{max}.

DRP-104 Treatment *In Vivo* Results in Dramatic Modulation of Multiple Relevant Direct Tumor and Immune Cell Related Scores as Measured by Nanostring® IO360 and Metabolism Panels

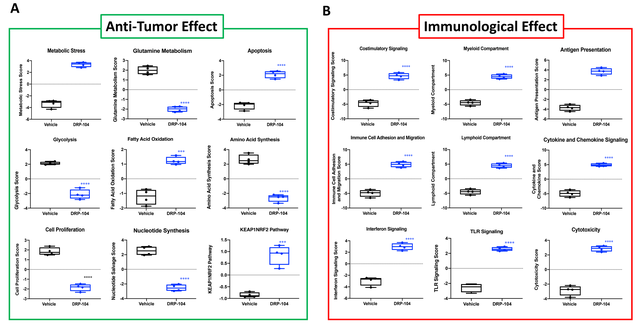

C

Metabolism Panel

Metabolism	Undirected Group: differential expression in Vehicle vs. baseline of DRP-104
Lysosomal Degradation	6.179
Glucose Transport	6.04
TLR Signaling	5.232
Glutamine Metabolism	5.104
Myc	4.777
Glycolysis	4.492
Vitamin & Cofactor Metabolism	4.48
Antigen Presentation	4.429
Fatty Acid Synthesis	4.399
Amino Acid Synthesis	4.056
Nucleotide Salvage	3.694
Nucleotide Synthesis	3.664
Endocytosis	3.535
Fatty Acid Oxidation	3.184
KEAP1/NRF2 Pathway	3.114
Amino Acid Transporters	3.109
Pentose Phosphate Pathway	3.055
Cytokine & Chemokine Signaling	2.98
NF-kB	2.946
Mitochondrial Respiration	2.873
Arginine Metabolism	2.816
TCR & Costimulatory Signaling	2.777
Reactive Oxygen Response	2.702
PI3K	2.639
Hypoxia	2.631
AMPK	2.497
MAPK	2.39
Cell Cycle	2.294
Transcriptional Regulation	2.209
Autophagy	2.127
mTOR	2.059
DNA Damage Repair	1.949
Tryptophan/Kynurenine Metabolism	1.742
Epigenetic Regulation	1.655
p53 Pathway	1.519
IDH1/2 Activity	1.488

IO360

IO360	Undirected Groups: differential expression in DRP-104 vs. Vehicle
Costimulatory Signaling	8.61
Myeloid Compartment	8.494
Antigen Presentation	8.473
Immune Cell Adhesion and Migration	8.326
Lymphoid Compartment	7.944
Cytokine and Chemokine Signaling	7.394
Hypoxia	7.372
JAK-STAT Signaling	7.268
Interferon Signaling	7.024
Cytotoxicity	6.699
NF-kappaB Signaling	6.577
PI3K-Akt	6.44
TGF-beta Signaling	6.272
Metabolic Stress	6.107
Matrix Remodeling and Metastasis	5.869
MAPK	5.835
Autophagy	5.6
Epigenetic Regulation	5.335
Wnt Signaling	5.001
Apoptosis	4.905
Hedgehog Signaling	4.863
Angiogenesis	4.527
Notch Signaling	4.51
Cell Proliferation	4.134
DNA Damage Repair	3.966

D

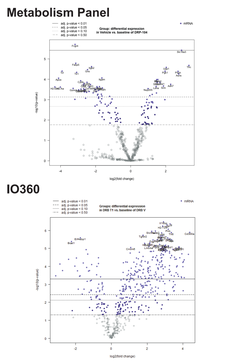

Figure 3. MC38 cells were inoculated *s.c.* in C57BL/6 mice. When tumor size reached ~400 mm^3, mice were treated with DRP-104 (0.5 mg/kg) or vehicle *s.c., q.d.* for 5 days in the opposite flank. mRNA was extracted from tumors and analyzed by Nanostring IO360 and Metabolism panels. **A.** Anti-tumor score, **B.** Immunological score, **C.** Modulation of scores, **D.** Volcano plots. ***: p<0.001 ****: p<0.0001.
DRP-104 treatment was associated with dramatic modulation of multiple relevant tumor and immune cell scores suggesting direct anti-tumor effects while stimulating immune cell function.

DRP-104 Administration Yields Dose-Dependent Changes in Key Tumor & Plasma Pharmacodynamic Metabolites

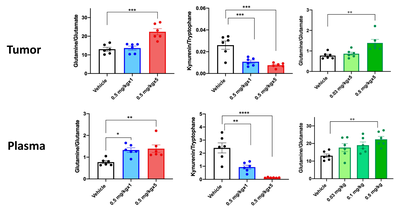

Figure 4. C57BL/6 mice bearing established MC38 tumors in the flank were dosed *s.c.* in the opposite flank with DRP-104 for one day or 5 consecutive days.*: p<0.05 **: p<0.01; ***: p<0.001, ****: p<0.0001.
Consistent and significant dose-dependent changes in tumor and plasma glutamine and glutamate pharmacodynamic metabolites were seen demonstrating target engagement of DRP-104. Modulation of Kynurenine/Tryptophan metabolism suggests DRP-104 may have additional impact on immune cell function in the TME.

DRP-104 Treatment *In Vivo* Results in Increased Immune Cell Infiltration to Tumors as Measured by Nanostring® GeoMx Profiling

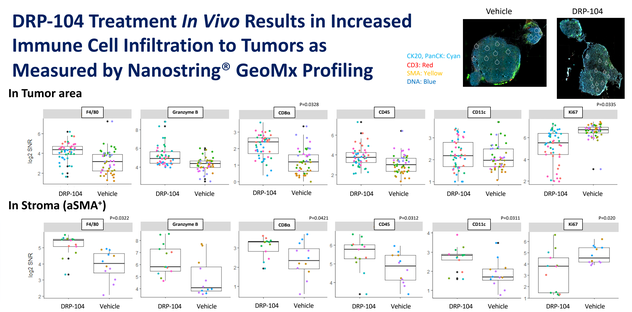

Figure 5. MC38 cells were inoculated *s.c.* in C57BL/6 mice. When tumor size reached ~400 mm^3, mice were treated with DRP-104 (0.5 mg/kg) or vehicle *s.c., q.d.* for 5 days in the opposite flank. Tumor tissues were processed for GeoMx ® Digital Spatial Profiler.
Significant increase of CD8a, decrease of Ki67, trend of increase of F4/80, Granzyme B, CD45, CD11c staining was observed in the tumor area. In the stroma area (aSMA+) a similar trend was observed plus significantly increased APCs (CD11c$^+$ DC and F4/80$^+$ macrophages) were seen.

DRP-104 Treatment Increases Activation and Infiltration of Immune Cells into Tumors *In Vivo*

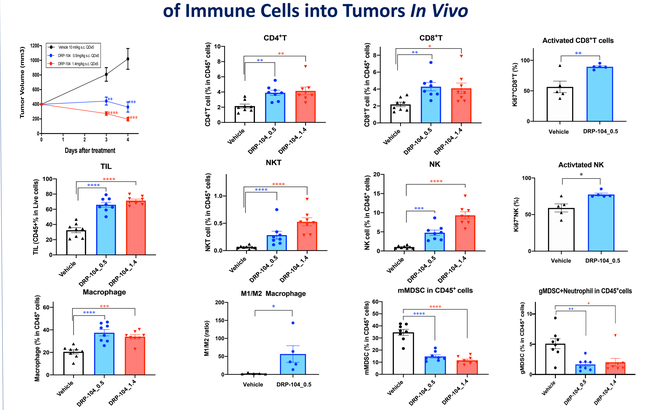

Figure 6. MC38 cells were inoculated *s.c.* in C57BL/6 mice. When tumor size reached ~400 mm^3, mice were treated with DRP-104 (0.5 or 1.4 mg/kg) or vehicle *s.c., q.d.* for 5 days in the opposite flank. Phenotypic analyses of tumor infiltrating immune cells and tumor cells were performed by flow cytometry. *: p<0.05; **: p<0.01; ***: p<0.001; ****: p<0.0001.
Increased tumor infiltration of activated T, NK and NKT cells with concomitant decrease in MDSCs was associated with anti-tumor activity suggesting DRP-104's MOA includes immuno-oncology effects.

Innate and Adaptive Immune Cells Contribute to DRP-104 Anti-Tumor Efficacy

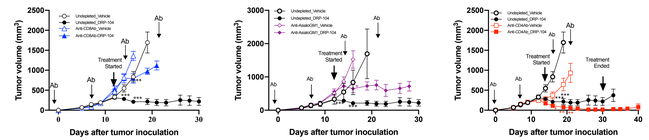

Figure 7. MC38 tumor bearing C57BL/6 mice were treated with anti-CD8$^+$Ab (**A**), anti-asialoGM1 Ab (**B**) or anti-CD4$^+$Ab (**C**) to deplete immune cells and then subsequently treated with DRP-104 0.5 mg/kg *s.c., qdx*5 days ON+2days OFFx3cycles or vehicle. n=5-10, **: p<0.01; ***: p<0.001.
CD8$^+$ cell depletion significantly reduced TGI. NK cell depletion lacked the early response of DRP-104 leading to partial reduction of TGI. CD4$^+$ cell depleted mice showed enhanced efficacy to DRP-104. These results indicate contribution of both innate and adaptive immune cells to the anti-tumor efficacy by DRP-104.

Combination of DRP-104 with Anti-PD-1 Ab or Anti-PD-L1 Ab Prolongs Animal Survival Compared to Single Agent Treatment

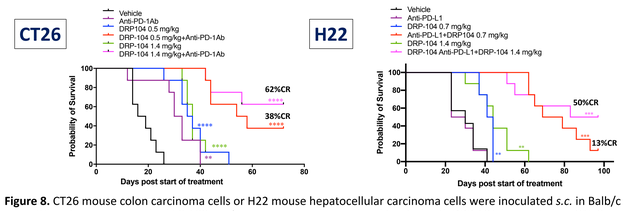

Figure 8. CT26 mouse colon carcinoma cells or H22 mouse hepatocellular carcinoma cells were inoculated *s.c.* in Balb/c mice. When tumor size reached 50-100 mm^3, mice were randomized and treated with DRP-104 (*sc, qdx*5 days ON+2days OFFx4cycles), anti-PD-1Ab (10 mg/kg, *ip, q4dx*8) or anti-PD-L1 Ab (5 mg/kg, *ip*, *q4dx*6), DRP-104+anti-PD-1Ab or anti-PD-L1 Ab combination. Days when tumor size reached >2000 mm^3 were plotted as survival endpoint. Animals that were identified to be tumor free >10 tumor volume doubling times after completion of drug treatment were considered as a durable cure. n=10, **: p<0.01; ***: p<0.001; ****: p<0.0001.
Anti-PD-1Ab in CT26 but not anti-PD-L1 Ab in H22 demonstrated survival effect. DRP-104 monotherapy achieved significant survival in both CT26 and H22 models. Combination of DRP-104 with anti-PD-1Ab or anti-PD-L1 Ab further extended the survival effect compared to single agent treatment and achieved long-term durable cures.

Conclusions

- DRP-104 achieved a 66x tumor/plasma ratio for DON in MC38 bearing CES-1 ko mice proving successful partitioning of prodrug to direct DON, the active moiety, to tumors.
- DRP-104 treatment yielded dose-dependent changes in key plasma & tumor metabolites, broad metabolomic reprogramming of the TME, and dramatic immuno-oncology related gene modulations. This was further supported by GeoMx® digital spatial profiling and Nanostring® gene expression analysis.
- Immuno-phenotypical analysis showed that DRP-104 induced substantial and broad changes in various immune cell infiltrates, such as increased TIL, T, NK and NKT cells. T cells and NK cells were more proliferative, TAMs were polarized to M1 phenotype, and MDSCs were decreased. All of these changes suggest broad remodeling of the TME by DRP-104 treatment.
- CD8$^+$ cell and NK cell depletion reduced TGI of DRP-104, while CD4$^+$ cell depletion enhanced anti-tumor efficacy of DRP-104 indicating an immune cell mediated anti-tumor mechanism of action.
- DRP-104 monotherapy demonstrated a prolonged survival effect in both CT26 and H22 models compared to immune checkpoint inhibitors. Combination of DRP-104 with either anti-PD-1 Ab or anti-PD-L1 Ab significantly increased efficacy, leading to long-term durable cures.

These data support clinical development of DRP-104 as a single agent and in combination with immune checkpoint inhibitors - including in settings of non-response to IO therapies. An IND has been recently opened and clinical development is forthcoming.